20-10-2004

Blur retrieval via separation of zeros sheets from noisy blurred images

Prashan Premaratne
University of Wollongong, prashan@uow.edu.au

I. Burnett
University of Wollongong, ianb@uow.edu.au

C. D. Liyanage
Massey University, New Zealand

Blur retrieval via separation of zeros sheets from noisy blurred images

Abstract

A novel method of separating the point spread function from blurred images using zeros of the Z transform is presented when more than one blurred image is available. The proposed method is demonstrated to be effective with significant contamination with signal-to-noise ratios of over 30 dB. This method holds much promise as a blind deconvolution (i.e. problem of recovering two functions from their convolution) technique, as it does not impose any constraints on the point spread function, such as positivity. The article is presented with experimental results over different signal-to-noise ratios, depicting its effectiveness as a practical image restoration technique.

Keywords

Z transforms deconvolution, image restoration, optical transfer function

Disciplines

Physical Sciences and Mathematics

Publication Details

This paper originally appeared as: Premaratne, P, Burnett, I and Liyanage, CD, Blur retrieval via separation of zeros sheets from noisy blurred images, Proceedings of 2004 International Symposium on Intelligent Multimedia, Video and Speech, 20-22 October 2004, 559-562. Copyright IEEE 2004.

Blur Retrieval via Separation of Zeros Sheets from Noisy Blurred Images

Prashan Premaratne, Ian Burnett* and C. D. Liyanage***

*School of Electrical, Computer & Telecommunications Engineering,
The University of Wollongong, Wollongong, NSW Australia 2500.
{prashan, i.burnett}@elec.uow.edu.au

**Institute of Information Sciences & Technology
Massey University, Palmerston North, New Zealand.

ABSTRACT

A novel method of separating point spread function from blurred images using zeros of the z transform is presented when more than one blurred images are available. The proposed method is demonstrated to be effective with significant contamination of signal-to-noise ratios over 30dB. This method holds much promise as a blind deconvolution (i.e. problem of recovering two functions from their convolution) technique, as it does not impose any constraints on the point spread function such as positivity. The article is presented with experimental results over different signal-to-noise ratios depicting its effectiveness as a practical image restoration technique.

1. INTRODUCTION

Blind image deconvolution has been demonstrated to be possible using the method of zero sheet separation [1], [2]. The authors have previously demonstrated a scheme where zero sheet separation is done effectively for practical sized images with point spread functions (PSF) having diagonal symmetry [3], [4], [5]. In this paper, we have attempted to extend this concept for generic PSFs when more than one blurred images are available from the same blurring system. This is a realistic scenario where a deep space probe might encounter two different scenes under similar circumstances, i.e., speed, imaging system setup etc. The technique is robust to noise contamination and still recovers the PSF reliably for signal-to-noise ratios over 30dB. This proves the versatility of the proposed schemes, as the above imaging scenario is inherent with noise contamination. Another advantage is that the technique does not need to incorporate any denoising techniques or iterative steps for reliable results in noise-corrupted images contrary to other research publications [6]. Since the PSF does not have any constraints such as positivity or non-singularity, the method can be treated as a more general blind image restoration technique. Furthermore, this technique is shown to obtain a more reliable estimate of PSF than Iterative Blind Deconvolution (IBD) [7] and simulated annealing [8], as it does not have any stability issues. The computational complexity involved in the whole process is minimal due to the row prediction formula [4].

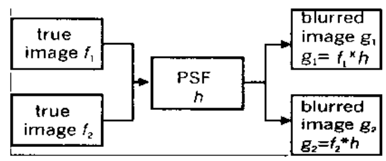

Figure 1: Blurring system with common PSF.

2. DERIVATION OF THE DEGRADATION MODEL

Let the true (original) images be denoted by $f_1(x,y)$, $f_2(x,y)$, the common PSF be given by $h(x,y)$ and the blurred images are denoted by $g_1(x,y)$ and $g_2(x,y)$. The blurring process can be expressed as

$$g_1(x,y) = f_1(x,y) * h(x,y) + n_1(x,y), \quad 0 \le x, y \le N + M - 1 \tag{1}$$

$$g_2(x,y) = f_2(x,y) * h(x,y) + n_2(x,y), \quad 0 \le x, y \le N + M - 1 \tag{2}$$

where $n_1(x,y)$ and $n_2(x,y)$ denote additive Gaussian noise in the system, * denotes 2-D convolution operator and the images are of size $N \times N$ and PSF is of size $M \times M$. Figure 1 depicts the blurring scenario outlined above in the absence of noise. If we allow the upper case letters represent the 2-D discrete Fourier transform (DFT) of their lower case counterparts and signal to noise ratio (SNR) is high such that we can ignore noise terms

$$G_1(k,l) = F_1(k,l)H(k,l), \quad 0 \le k, l \le N + M - 1. \tag{3}$$

$$G_2(k,l) = F_2(k,l)H(k,l), \quad 0 \le k, l \le N + M - 1. \tag{4}$$

From the definition of DFT G_1 can be expressed as

$$G_1(k,l) = \sum_{y=0}^{N+M-1} \sum_{x=0}^{N+M-1} g_1(x,y) e^{(-j2\pi(kx+ly)/(N+M-1))} \tag{5}$$

The finite degree 2-D z transform is obtained with the simple change of variables $u = \exp(-j2\pi k/(N+M-1))$ and $v = \exp(-j2\pi l/(N+M-1))$, G_1 and G_2 can be written as

$$G_1(u,v) = \sum_{y=0}^{N+M-1}\sum_{x=0}^{N+M-1} g_1(x,y)u^x v^y \quad (6)$$

$$G_2(u,v) = \sum_{y=0}^{N+M-1}\sum_{x=0}^{N+M-1} g_2(x,y)u^x v^y \quad (7)$$

Our systematic approach to deconvolution of expression (1) in the absence of noise is based on factoring the 2-D polynomial by manipulating the 1-D polynomials that is obtained from Equations (6) and (7) by writing complex coefficients based on $g_1(x,y)$, $g_2(x,y)$ and u. From Equations (6) and (7) it is easy to see that

$$G_1(u,v) = \sum_{y=0}^{N+M-1} a_y(u)v^y, \quad (8)$$

where $a_y(u) = \sum_{x=0}^{N+M-1} g_1(x,y)u^x$.

$$G_2(u,v) = \sum_{y=0}^{N+M-1} b_y(u)v^y, \quad (9)$$

where $b_y(u) = \sum_{x=0}^{N+M-1} g_2(x,y)u^x$.

From Equations (3) and (4) we can clearly see that z transforms $G_1(u,v)$ and $G_2(u,v)$ are composite of two zero sheets $F_1(u,v)$, $H(u,v)$ and $F_2(u,v)$, $H(u,v)$ respectively (assuming $f_1(x,y)$, $f_2(x,y)$ and $h(x,y)$ are irreducible). Since the equation (8) and (9) are one-dimensional polynomials of degree $N+M-1$, we can find $N+M-1$ roots that depend on the free parameter u. If particular values of u (say u_c's) are selected to correspond to rows of the blurred image matrix (convolution of image and PSF), $N+M-1$ such one-dimensional polynomials can be formed whose roots are known as point zeros. These zeros comprise point zeros of blurred image thus the union of PSF and true image zeros. This phenomenon can be observed using their excursions called zero tracks for the values of u, $v = 1.0exp(\phi)$ with $0 \le \phi < 2\pi$ [9]. Figures 2(a), 2(b) and 2(c) depict the zero tracks of image1, image2, and PSF respectively and figures 3(a) and 3(b) show the union of zero tracks. It is observable in this simple example that blurred image is in fact, a direct combination of individual zero tracks of true image and PSF. The zero tracks of blurred image comprise of 4 roots of image matrix (of size 5×5) and 2 roots of PSF (of size 3×3), thus the composite of the roots comprise of 6 roots. The two roots of the PSF create identical tracks in both figures 3(a) and 3(b) whereas, the image matrix has different root excursions in them due to different imaged scenes.

Figures 4(a) and 4(b) show the changes in above zero tracks in the presence of noise contamination amounting to Blur Signal-to-Noise Ratio (BSNR) of 30dB. Figures 3(a) and 4(a) show minor differences in their zero tracks and this does not pose a major obstacle in the recovery of PSF, as would be discussed in next section.

Since the PSF is common to both blurred images, the point zero composites of both blurred images contain matching zeros, which belong to the PSF. Identification of these zeros and the consequent construction of 1-D polynomials can be used to form the DFT matrix of the PSF. Taking the inverse DFT of this would result in recovery of PSF. However, identification of the correct M rows of PSF is not trivial. This is the case since matching of zero sheets of size $(M+N-1)\times(M+N)$ (polynomial of order $M+N-1$ has $M+N$ zeros or roots) would produce $(M+N-1)\times(M-1)$ sized zero sheet for the PSF. Out of these $M+N-1$ rows only correct M rows would produce the desired DFT of the PSF. In most instances, free parameter u assuming row values (that is to say u assuming integer values corresponding to rows) may not yield proper polynomials at all. The u values should have fractional increments in between row values. Hence, the exact u (increment step) value and the corresponding row number are given by the row prediction formula as follows [4].

$$\text{Row Number} = n\left(\frac{V}{M}\times\frac{1}{i}\right) \quad (10)$$

where $n = 0,1,2,..$, PSF is of size $M\times M$, the convolution size is $V = M+N-1$ and for an increment step size (e.g. $u = 0.1$) denoted by i, the row number to be admitted is given by expression (10). It is important that row number yields an integer value for a realistic row. This is achieved by adjusting the increment step value i. Moreover, it is imperative to select a larger enough i, satisfying the above conditions to avoid unnecessarily large matrices to process. This fact can be illustrated by referring to table 2. This zero sheet is generated with $i = 7/9$ and only the highlighted rows produce the corresponding polynomials for PSF recovery. However, the point zero rows of the blurred images evaluated independently of one another varies from their true value by a complex constant [10].

Referring back to equations (6) and (7), 2-D polynomials were transformed to 1-D polynomials in equations (8) and (9) by treating u as constants for corresponding row values. Exchanging the roles of u and v, where v corresponds to columns of the matrices, another set of equations can be derived. Following a similar procedure as described above for the recovery of PSF, new DFT of PSF (this is not a valid DFT as the columns have been formed independently) can be formed. However, it is now obvious that these two DFT versions of PSF are in fact the same if their rows and columns have the right multiplication ratio. Let the $M\times M$ inverse discrete Fourier transform (IDFT) matrix be denoted by $\mathbf{T}$, PSF formed row-vice and column-vice are denoted by $\mathbf{H_R}$ and $\mathbf{H_C}$, respectively. Supposing vector $\mathbf{A}$ denotes the ratio needed to be applied to the independently evaluated rows

of $\mathbf{H_R}$ such that it forms the true DFT of the PSF, the following expressions can be obtained.

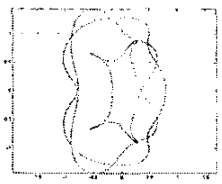
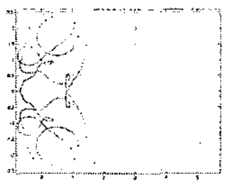

Figure 2(a) Figure 2(b)

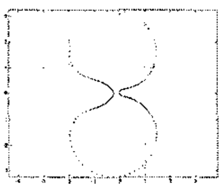

Figure 2(c)
(2a) Zero tracks of image 1.
(2b) Zero tracks of image 2.
(2c) Zero tracks of PSF.

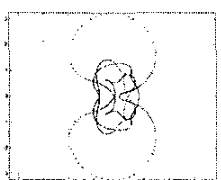
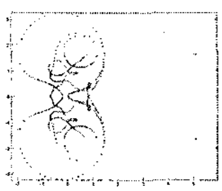

Figure 3(a) Figure 3(b)
(3a) Zero tracks of blurred image 1.
(3b) Zero tracks of blurred image 2.

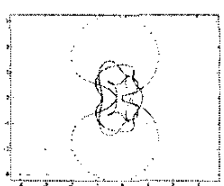
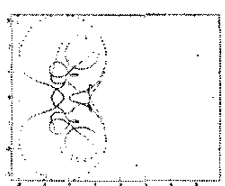

Figure 4(a) Figure 4(b)
Zero tracks of the blurred images with noise

$$A' = [1 \quad r_2 \quad r_3 \quad . \quad . \quad . \quad r_M]$$

$$h = \mathbb{C}_1 T(A \bullet * H_R) \tag{11}$$

$$A \bullet * H_R = \begin{bmatrix} 1 & a_{12} & a_{13} & . & a_{1M} \\ r_2 & r_2.a_{22} & r_2.a_{23} & . & r_2.a_{2M} \\ r_3 & r_3.a_{32} & . & . & . \\ . & . & . & . & . \\ r_M & r_M.a_{M2} & . & . & r_M a_{MM} \end{bmatrix} \tag{12}$$

where A^t denotes the transpose of **A** and r_1 is chosen to be 1 and '•*' denotes column-vice multiplication such that multiplication of **A** and $\mathbf{H_R}$ yields equation (12). Furthermore, $\mathbb{C}_1$ denotes a complex constant in general which accounts for the deviation of the recovered PSF matrix from true **h**. With a similar approach having **B** denoting a vector, which is the ratio needed to be applied to the independently evaluated columns of $\mathbf{H_C}$ such that it forms the true DFT of the PSF, the following expressions can be obtained.

$$B = [1 \quad c_2 \quad c_3 \quad . \quad . \quad . \quad c_M]$$

$$B \circ * H_C = \begin{bmatrix} 1 & c_1 & c_2 & . & c_M \\ b_{21} & c_1.b_{22} & c_2.b_{23} & . & c_M.b_{2M} \\ . & & & & . \\ . & & & & . \\ b_{M1} & c_1.b_{M2} & . & . & c_M b_{MM} \end{bmatrix} \tag{13}$$

where '∘*' denotes row-vice multiplication such that multiplication of **B** and $\mathbf{H_C}$ yields equation (13). Now the PSF, calculated using independent evaluation of columns could be stated as

$$h = \mathbb{C}_2 (B \circ * H_C)' T' \tag{14}$$

Thus equating expressions (11) and (14) and letting $\mathbb{C} = \mathbb{C}_2 / \mathbb{C}_1$ would result in

$$T(A \bullet * H_R) = \mathbb{C}(B \circ * H_C)' T' \tag{15}$$

Since **T**, $\mathbf{H_R}$, and $\mathbf{H_C}$ are known, complex constant $\mathbb{C}$, ratio vectors **A** and **B** could be found by solving equating matrix elements) any $2M$-1 out of $M \times M$ equations. The next section describes some of the simulation results using these theoretical developments.

(a)

6.0000	1.9999	2.9985
-6.0086	1.9989	4.0026
2.0053	2.9993	0.9975

(b)

6.0000	1.9996	2.9989
-6.0015	1.9993	4.0006
2.0002	2.9994	0.9993

(c)

6.0000	1.9997	3.0000
-6.0019	1.9999	4.0002
2.0015	2.9999	0.9995

(d)

6.0000	1.9999	3.0000
-6.0005	1.9999	4.0000
2.0004	2.9999	0.9998

Table 1: Recovered PSF with different noise contamination levels: (a) BSNR= 31 dB, (b) BSNR= 40.5 dB (c) BSNR= 50 dB, and (d) BSNR = 60.5 dB.

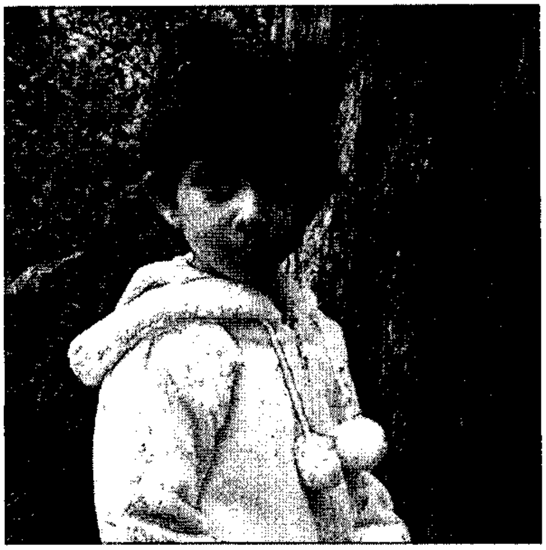

Figure 5. Original image of size 512x512

Figure 6. Blurred image with noise (BSNR = 21dB)

3. SIMULATION RESULTS

We used a 3×3 PSF ([6 2 3; -6 2 4; 2 3 1]) and two 5×5, 8-bit gray scale images. The first simulation was performed without additive noise and recovered the exact PSF using the proposed scheme. The second phase of the simulations involved varying amount of noise levels, BSNR ranging from 30dB to 60dB. The process retrieved good estimations of PSF. As can be seen from the table 1, very high accuracy was possible for higher BSNR ratios. Even at moderate BSNR level of 30dB, accuracy of the recovered PSF is high enough for most practical usage. Figures 5 and 6 show results obtained using real images of size 512x512 with a BSNR of 21dB. The accuracy was lower than the results obtained in Table 1.

4. CONCLUSION

Separation of zero sheets for blind image deconvolution holds lot of promise for future research due to its simplicity in visualizing zero tracks for small images. However, for practical sized images, visualization of zero tracks does not convey any useful information as it involves many hundreds of zero tracks. The interesting aspects of the developments in this research are that PSF recovery is achieved via direct non-iterative process involving no stability issues. Furthermore, it does not assume any parametric form or positivity constraints for PSF. Yet, it is very robust to noise contamination.

5. REFERENCES

[1] D.C. Ghiglia, L.A. Romero and G.A. Mastin, "Systematic Approach To Two-Dimensional Blind Deconvolution By Zero-Sheet Separation", *J. Opt. Soc. Am. A.*, vol. 10-5, pp. 1024-1036, 1993.

[2] R.G. Lane, and R.H.T. Bates, "Automatic Multidimensional Deconvolution", *J. Opt. Soc. Am.*, vol. 4-1, pp. 180-188, 1987.

[3] P. Premaratne and C. C. Ko, "Zero Sheet Separation Of Blurred Images With Symmetrical Point Spread Functions" *in Proc. Thirty-third Asilomar Conference on Signals, Systems, and Computers*, vol. 2, pp. 1218-1220.

[4] P. Premaratne, and C. C. Ko, "Retrieval of Symmetrical Image Blur using Zero Sheets", *Proceedings of IEE Vision, Image and Signal Processing*, vol. 148-1, pp. 65-69, 2001.

[5] Premaratne, P. and M. Premaratne, "Accelerated Iterative Blind Deconvolution of Still Images", in Proc. of Conference on Convergent Technologies for Asia-Pacific Region TENCON 2003 , vol. 1 , pp. 6-10, 2003.

[6] B.L.K. Davey, R.G. Lane and R.H.T. Bates, "Blind Deconvolution Of Noisy Complex-Valued Images", *Opt. Commun.*, vol. 69-5,6, pp. 353-356, 1989.

[7] G.R. Ayers, and J.C. Dainty, "Iterative Blind Deconvolution Method And Its Applications", *Optics Lett.*, vol. 13-7, pp. 547-549, 1988.

[8] B.C. McCallum, "Blind Deconvolution By Simulated Annealing", *Optics Commun.*, vol. 75-2, pp. pp. 101-105, 1990.

[9] R.W. Watson, C.R. Parker and P.J. Bones, "Demonstration Of Two-Dimensional Consistent Deconvolution Using Zeros", *Opt. Commun.*, vol. 93-5,6, pp. 359-365, 1992.

[10] P.J. Bones, Parker, C.R., Satherley, B.L., and R.W. Watson, "Deconvolution And Phase Retrieval With Use Of Zero Sheets", *J. Opt. Soc. Am.*, vol. 12, pp. 1842-1857, 1995.